Nonlinear Electromechanical Interactions in Rotordynamics of Electrical Machines

Felix Boy*, Hartmut Hetzler*

Institute of Mechanics - Engineering Dynamics Group, University of Kassel, Kassel, Germany

<u>Summary</u>. Within this contribution the modelling of nonlinear electromechanical interaction in electrical machines is revised regarding to rotordynamics. Hereto an existing analytical approach to solve the magnetic field problem in the air gap of a machine with eccentrically running rotor is extended towards arbitrary machine design. The task is solved by finding an exact solution of the field problem in the air gap domain using bipolar coordinates. The results of the magnetic field, the magnetic energy and forces are obtained as a Fourier series with an iterative algorithm to calculate the involved coefficients. Practical applicability is shown by a study comparing the series expansion to a finite element solution. It turns out, that the series converges very fast even if realistic boundary conditions are applied.

Introduction

Electrical machines are of huge technological interest: Their large range of application, their variety and quantity outline the necessity to better understand the underlying physical principles. Especially for machines with high running speeds, vibration problems due to eccentrically running rotors become a major issue. Among them are questions on reliability [1], on sound and comfort [2] and on system state monitoring [3]. Understanding these phenomena and predicting the machine behaviour requires an exact but still efficient dynamical machine model. It is the aim of this work to contribute to establish such a model.

Apart from mechanical aspects like unbalance and bearing dynamics, the main cause of vibration in electrical machines is the electromechanical interaction mediated by the magnetic field. It exerts magnetic forces and torque and induces voltage to the electrical circuits. In return, the mechanical motion and the currents flowing in the circuits affect the field itself, such that one finds a complex multiphysical system (figure 1) which is likely to exhibit all kinds of oscillatory phenomena.
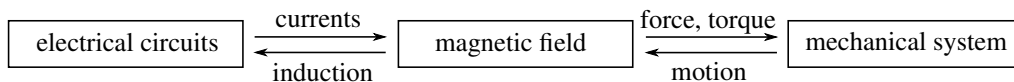

Figure 1: Abstract model of an electromechanical machine involving three subproblems and coupling.

From a theoretical point of view, a dynamical analysis of a lumped parameter model for the mechanical system and the electrical circuits can be carried out, if the magnetic co-energy $W_m^*(\boldsymbol{x}, \boldsymbol{i})$ is known analytically, depending on the mechanical state $\boldsymbol{q} \in \mathbb{R}^{n \times 1}$ and the electrical currents $\boldsymbol{i} \in \mathbb{R}^{m \times 1}$. Finding this co-energy presumes solving a magnetic field problem in the iron parts and the air gap of the machine. While both stator and rotor material are magnetically nonlinear and therefore hard to handle analytically, the field problem in the air gap is linear and thus accessible for an analytical solution. The advantages of such a solution in the air gap are an exact knowledge of the electromagnetic force and flux linkages depending on the system statevector $(\boldsymbol{q}, \boldsymbol{i})^\top$ avoiding known issues with numerical force computation and mesh deformation [4].

In literature there are many different approaches to solve the considered problem. This contribution is focussed on analytical methods and may only discuss some of them. Starting from earlier graphical methods, as for example used by Rosenberg in 1917 [5], most frequently applied methods are based on approximation or linearisation. In this context, there is a vast majority using the so called permeance-harmonic-method [1,6-11]. Here one assumes a purely radially orientated magnetic field and finds the field solution by multiplying the magnetomotive force (boundary condition) by the so called air gap permeance [7]. It can be shown by asymtotic analysis [12] that the permeance-harmonic-method involves an error of order $\mathcal{O}(\frac{\delta_m}{r_2})$ compared to the exact solution, where δ_m is the air gap width for a centrically running rotor and r_2 is the rotor radius. Furthermore, most publications linearise the air gap permeance with respect to the mechanical state $\boldsymbol{q}$ and are therefore restricted to linear rotordynamical analysis.

Besides that, exact nonlinear solutions have been established for special cases of the boundary conditions by Buchholz in 1933 [13] using conformal mapping and a complex scalar potential, as well as by Skubov and Shumakovich in 1999 [14] with bipolar coordinates and a magnetic vector potential. While the work by Buchholz involves some quite advanced technique and his solution is rather cumbersome, the approach by Skubov and Shumakovich seems suitable for a general application in the field of rotordynamics of electrical machines.

As the solution given by Skubov and Shumakovich is restricted to two pole machines regarding only fundamental harmonics in the boundary condition, it is the aim of this work to extend the approach towards any machine design involving arbitrary boundary conditions. Furthermore, this study proves the applicability of the method towards fully coupled dynamical analysis showing the convergence of the involved series compared to a FE-solution.

Subsequently, in section 2 of this contribution, the field problem is stated and the analytical solution found in the work of Skubov and Shumakovich is revised and extended. In the third section, realistic boundary conditions and the numerical model are presented and the convergence of the analytical solution is verified for a representative example of a 4-pole

cage induction machine. The discussion concludes with a summary and an outlook on possible semi-analytical extensions of the proposed approach.

Model

Stating the field problem in the air gap domain Ω (see figure 2 a), the derivation starts from Ampère's and Gauß' law

$$\nabla \times \vec{H} = \vec{0}, \tag{1}$$

$$\nabla \cdot \vec{B} = 0. \tag{2}$$

Here, $\vec{H}$ is the magnetic field and $\vec{B}$ is the magnetic induction. Note that there is no current density within the air gap domain. The corresponding boundary conditions for the magnetic field are

$$\vec{n} \times \vec{H}\Big|_{\partial \Omega_i} = -\vec{k}_i, \quad i = 1, 2 \tag{3}$$

at the boundaries $\partial \Omega_1$ and $\partial \Omega_2$, where $\vec{n}$ denotes the surface outer normal and $\vec{k}_1$ and $\vec{k}_2$ are surface current densities, respectively.
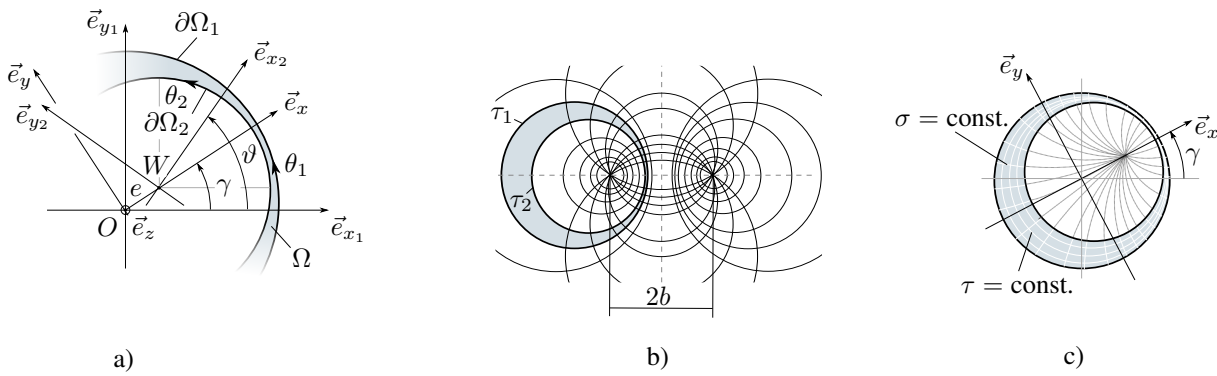

a) b) c)

Figure 2: Kinematics and bipolar coordinates for the eccentric annulus problem.
      a) Kinematics of the eccentrically running rotor and definition of coordinate systems.
      b) Transformation to bipolar coordinates
      c) Illustration of bipolar coordinates in the corotating frame of reference.

According to Helmholtz' theorem each sufficently smooth, rapidly decaying vector field can be decomposed into a curl-free and a divergence-free vector field. Applied to the magnetic induction, this implies

$$\vec{B} = \nabla \times \vec{A} - \mu_0 \nabla \mathcal{V}, \tag{4}$$

where $\vec{A}$ is a vector potential, μ_0 is the magnetic field constant and $\mathcal{V}$ is a scalar potential. The factor $-\mu_0$ makes the derivation consistent to publications using a scalar potential (e.g. [12, 13]) but is not necessary.
For the air gap the constitutive law relating $\vec{B}$ and $\vec{H}$ reads

$$\vec{B} = \mu_0 \vec{H}, \quad \Rightarrow \vec{H} = \frac{1}{\mu_0} \nabla \times \vec{A} - \nabla \mathcal{V}. \tag{5}$$

Inserting eq. (4) into (2) and (5) into (1) yields the field equations

$$\Delta \mathcal{V} = 0, \tag{6}$$

$$\Delta \vec{A} = \vec{0}, \tag{7}$$

in Ω, where the Coulomb gauge $\nabla \cdot \vec{A} = 0$ has been applied.

Concerning the boundary conditions eq. (5) is inserted into eq. (3). Rearranging and solving for the air gap potentials results in

$$\vec{n} \times (\frac{1}{\mu_0} \nabla \times \vec{A} - \nabla \mathcal{V})\Big|_{\partial \Omega_i} = -\vec{k}_i. \tag{8}$$

As the problem is considered to be planar, one is free to either use the vector potential $\vec{A}$ or the scalar potential $\mathcal{V}$ to fulfil these conditions. In this contribution, the vector potential shall be chosen, prescribing

$$\vec{A} = A(\vec{r}, t)\vec{e}_z, \quad \mathcal{V} = \mathcal{V}_0(t), \tag{9}$$

where $\vec{r}$ is the position vector to a certain point in the air gap domain Ω. The spatially constant part $\mathcal{V}_0(t)$ in the scalar potential accounts for homopolar fluxes and can be determined as described by Belmans [9]. Thus the boundary conditions become

$$\vec{n} \times \nabla \times \vec{A} \Big|_{\partial\Omega_i} = -\mu_0 \vec{k}_i. \tag{10}$$

The solution of the field equation for $\vec{A}$ can be calculated using bipolar coordinates as proposed by Skubov and Shumakovich [14]. The advantage of this kind of coordinates lies in the fact, that separation can be applied to the Laplace operator, as well as to the boundary conditions. This would not be possible using cylinder or cartesian coordinates. As a matter of fact, the solution to Laplace's equation on an eccentric annulus as a mathematical problem is well known [15]. It has been applied to many kinds of physical problems, as for example by Heyda on an incompressible flow between non-concentric cylinders [16].

Deriving the solution demands for a proper definition of different frames of reference and the transformation to bipolar coordinates. Consider figure 2 a: it depicts a part of the eccentric annulus air gap region Ω. The rotor is located eccentrically and its shaft centre position (point W) is described by the eccentricity e and phase angle γ with respect to the spacially fixed stator frame of reference $\mathcal{K}_1 = \{O, [\vec{e}_{x_1}, \vec{e}_{y_1}, \vec{e}_{z_1}]\}$. The moving frame $\mathcal{K}_\delta = \{O, [\vec{e}_x, \vec{e}_y, \vec{e}_z]\}$ is fixed to the origin O and its $\vec{e}_x$-axis points towards the position of the smallest air gap (direction of eccentricity). A second corotating frame $\mathcal{K}_2 = \{W, [\vec{e}_{x_2}, \vec{e}_{y_2}, \vec{e}_{z_2}]\}$ is attached to the shaft centre W: its orientation is described by ϑ against $\vec{e}_{x_1}$. Introducing polar coordinates $(r_i, \theta_i, z), i = 1, 2$ as shown in figure 2 a, the boundary conditions can be written as

$$\frac{\partial A}{\partial r_1}\Big|_{\partial\Omega_1} = \mu_0 k_1 \quad \text{and} \quad \frac{\partial A}{\partial r_2}\Big|_{\partial\Omega_2} = \mu_0 k_2, \tag{11}$$

where the functions $\vec{k}_1 = k_1(\theta_1)\vec{e}_z$ and $\vec{k}_2 = k_2(\theta_2)\vec{e}_z$ are periodic with respect to θ_1 and θ_2. Finding them from a given machine winding design is a basic task described in many textbooks (e.g. [17]) and will be outlined shortly within the results section.

Having introduced basic kinematics, the derivation continues with defining bipolar coordinates $\tau \in \mathbb{R}$ and $\sigma \in [-\pi, \pi)$ within $\mathcal{K}_\delta$, as shown in figure 2 b and c. Differing from the definition in classical textbooks and in the work by Skubov and Shumakovich [14], they are be defined as

$$x = -b\frac{\sinh\tau}{\cosh\tau - \cos\sigma} + \sqrt{R_1^2 + b^2}, \quad y = b\frac{\sin\sigma}{\cosh\tau - \cos\sigma},$$

$$\text{with} \quad 2b = \sqrt{\frac{[(R_1 + R_2)^2 - e^2][(R_1 - R_2)^2 - e^2]}{e^2}}. \tag{12}$$

Here R_1 and R_2 are the stator bore and rotor radius respectively and $2b$ is a geometrical parameter describing the distance between the coordinate foci (figure 2 b). This definition provides a proper matching to the given problem: The negative sign in x accounts for the inversion of coordinates in the $\vec{e}_x$-direction, as the region left of the axis of symmetry in figure 2 c is considered. The term $\sqrt{R_1^2 + b^2}$ shifts the coordinate origin to the stator centre.

As one can easily see, the coordinate transformation is singular for $e \to 0$. However, the magnetic co-energy, calculated forces and flux linkages which are the only relevant quantities for a dynamical analysis, such that the approach is not restricted to $e \neq 0$.

As mentioned before, the Laplace operator in eq. (7) is invariant with respect to the given coordinate transformation, so the solution can be found using separation. It is

$$A = \mu_0 \sum_{n=1}^\infty \frac{\cosh(n(\tau - \tau_2))}{n\sinh(n(\tau_2 - \tau_1))}\left[\Gamma_{Cn}^{(1)}\cos(n\sigma) + \Gamma_{Sn}^{(1)}\sin(n\sigma)\right]$$

$$+ \frac{\cosh(n(\tau - \tau_1))}{n\sinh(n(\tau_2 - \tau_1))}\left[\Gamma_{Cn}^{(2)}\cos(n\sigma) + \Gamma_{Sn}^{(2)}\sin(n\sigma)\right], \tag{13}$$

where τ_1 and τ_2 are the values of coordinate τ at the region borders and

$$\Gamma_{Cn}^{(i)} = \frac{1}{\pi}\int_{-\pi}^{\pi}\frac{b\, k_i(\theta_i)\cos(n\sigma)}{\cosh\tau_i - \cos\sigma}\, d\sigma \quad \text{and} \quad \Gamma_{Sn}^{(i)} = \frac{1}{\pi}\int_{-\pi}^{\pi}\frac{b\, k_i(\theta_i)\sin(n\sigma)}{\cosh\tau_i - \cos\sigma}\, d\sigma, \qquad i = 1, 2 \tag{14}$$

are corresponding Fourier coefficients. The boundary conditions k_i can be expressed as Fourier series

$$k_i(\theta_i) = \sum_{\nu=1}^{\infty} c_\nu^{(i)} \cos(\nu\theta_i) + s_\nu^{(i)} \sin(\nu\theta_i). \tag{15}$$

Skubov and Shumakovich [14] solved the integrals in eq. (14) for $\nu = 1$ and $\nu = 2$ in closed form. In this contribution the integrals are solved for all $\nu \in \mathbb{N}$, as described in detail in the appendix. The result is

$$\Gamma_{Cn}^{(i)} = -\frac{b}{\sinh \tau_i} \sum_{\nu=0}^{\infty} c_\nu^{(i)} \mathcal{C}_{\nu,n}^{(i)}, \quad \Gamma_{Sn}^{(i)} = -\frac{b}{\sinh \tau_i} \sum_{\nu=0}^{\infty} s_\nu^{(i)} \mathcal{S}_{\nu,n}^{(i)}, \tag{16}$$

where the coefficients

$$\mathcal{C}_{\nu,n}^{(i)} = \frac{1}{\pi} \int_{-\pi}^{\pi} \cos(\nu\theta_i) \cos(n\sigma) \, \mathrm{d}\theta_i \quad \text{and} \quad \mathcal{S}_{\nu,n}^{(i)} = \frac{1}{\pi} \int_{-\pi}^{\pi} \sin(\nu\theta_i) \sin(n\sigma) \, \mathrm{d}\theta_i \tag{17}$$

are integral expressions solved iteratively by

$$\mathcal{C}_{\nu,0}^{(i)} = 0, \quad \mathcal{C}_{\nu,1}^{(i)} = -2 \sinh \tau_i \, e^{-\nu\tau_i},$$

$$\mathcal{C}_{\nu,n}^{(i)} = 2(\cosh \tau_i - \frac{\nu}{n-1} \sinh \tau_i) \, \mathcal{C}_{\nu,n-1}^{(i)} - \mathcal{C}_{\nu,n-2}^{(i)} \qquad \forall n > 1. \tag{18}$$

$$\mathcal{S}_{\nu,n}^{(i)} = -\mathcal{C}_{\nu,n}^{(i)}$$

With this solution, it is easy to find the magnetic co-energy coinciding with the magnetic energy, defined by

$$W_m^* = \frac{\ell}{2} \sum_{i=1}^{2} \int_{\partial\Omega_i} \vec{A} \cdot \vec{k}^{(i)} \, \mathrm{d}S, \tag{19}$$

where ℓ is the axial air gap length. Inserting eqs. (13) and (15) into (19) leads to

$$W_m^* = \frac{\mu_0 \pi \ell}{2} \sum_{n=1}^{\infty} \frac{\cosh(n(\tau_1 - \tau_2))}{n \sinh(n(\tau_2 - \tau_1))} \left[\Gamma_{Cn}^{(1)\,2} + \Gamma_{Sn}^{(1)\,2} \right] + \frac{2}{n \sinh(n(\tau_2 - \tau_1))} \left[\Gamma_{Cn}^{(1)} \Gamma_{Cn}^{(2)} + \Gamma_{Sn}^{(1)} \Gamma_{Sn}^{(2)} \right]$$

$$\frac{\cosh(n(\tau_1 - \tau_2))}{n \sinh(n(\tau_2 - \tau_1))} \left[\Gamma_{Cn}^{(2)\,2} + \Gamma_{Sn}^{(2)\,2} \right]. \tag{20}$$

Having found the magnetic co-energy, forces and torque are calculated by

$$F_e = \frac{\partial W_m^*}{\partial e}, \quad F_\gamma = \frac{1}{e} \frac{\partial W_m^*}{\partial \gamma} \quad \text{and} \quad T_\vartheta = \frac{\partial W_m^*}{\partial \vartheta}. \tag{21}$$

Here F_e points towards the smallest air gap and is usually denoted as unbalanced magnetic pull (UMP), F_γ points perpendicularly to F_e and T_ϑ is the exhibited torque between rotor and stator. Similarly forces and torque in other frames of reference can be calculated by $\boldsymbol{F} = \frac{\partial W_m^*}{\partial \boldsymbol{x}}$ and flux linkages by $\boldsymbol{\Psi} = \frac{\partial W_m^*}{\partial \boldsymbol{i}}$.

Results

The expressions derived in section 2 shall now be verified by comparing them to a FE-computation, assessing their convergence when the series is truncated for certain finite (ν, n). In this survey the magnetic co-energy W_m^* as a quadratic form in $\vec{H}$ and its derivative with respect to the eccentricity, the UMP F_e, are used as measures of convergence. As a benchmark problem for the verification, a fixed instance in time in a simple 4-pole cage induction machine shall be considered, where the currents in the stator slots and rotor bars are prescribed. Following classical analytical approaches [7], boundary conditions in terms of so called current sheets for the air gap field problem are derived.
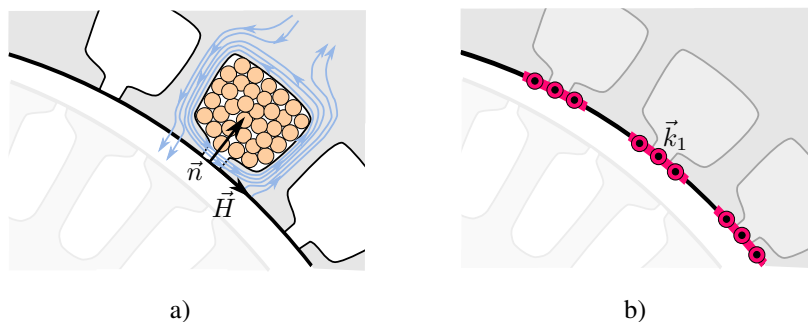

a)   b)

Figure 3: Derivation of boundary conditions by analytical means: definition of local current sheets.

For this purpose cosider figure 3 a, which illustrates an exemplary winding design of an asynchronous machine. One single stator slot is highlighted and shown in detail. The currents i_1, flowing in the conductors, evoke a circulating H-field surrounding the slot. As the scetch indicates, field lines at the slot opening are nearly parallel to the stator bore surface. Thus, considering eq. (3) one can find the boundary condition $\vec{k}_1 = \frac{N_1 i_1}{\ell_{s1}}\vec{e}_z$ in that region by defining an artificial current sheet of length ℓ_{s1} smearing all N_1 currents i_1 on to a narrow strip on the surface (figure 3 b).
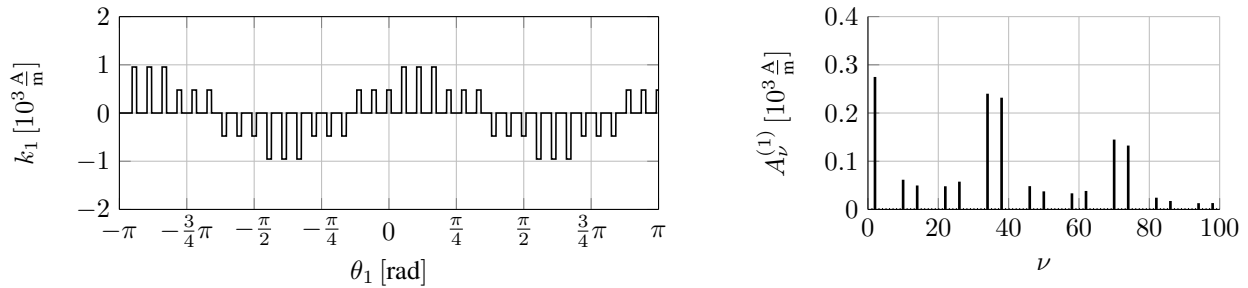

Figure 4: Current sheet and spectrum at the stator bore surface

At regions in between the slots, the field trespasses the surface nearly perpendicularly (no tangential component) making the current sheet a step like distributed function as shown on the left in figure 4. The argumentation for the rotor surface is analogous and its current sheet is shown in figure 5. As both boundary functions are periodic with respect to the circumferencial coordinate, they can be expressed in terms fourier series as mentioned earlier. The spectra of their amplitudes defined by

$$A_\nu^{(i)} = \sqrt{(c_\nu^{(i)})^2 + (s_\nu^{(i)})^2} \tag{22}$$

are shown on the right of figures 4 and 5.

As it can be seen in the spectra, the convergence of amplitudes $A_\nu^{(i)}$ towards zero with rising order ν is quite slow, as the current sheet distribution has a sharp rectangular shape. While one can easily identify a clean three phase current system at the stator, the currents in the rotor bars are defined according to a typical running condition, where eccentricity and induction cause an alteration of the current spectrum in terms of side bands. These are known to cause lateral magnetic forces [1].
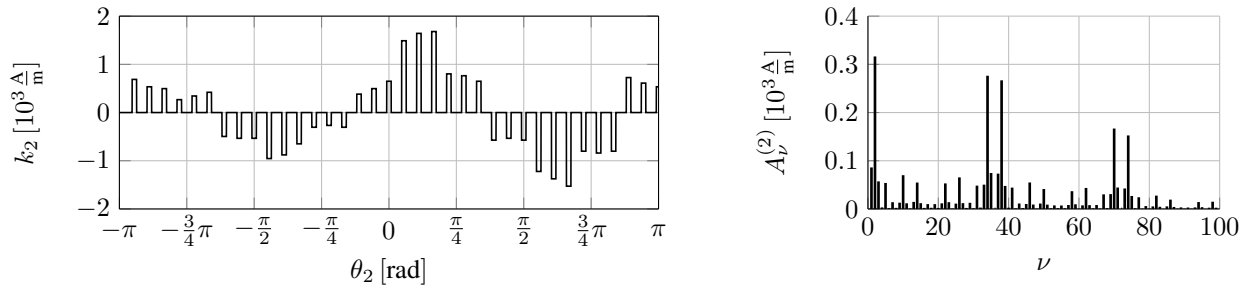

Figure 5: Current sheet and spectrum at the rotor surface

Furthermore, some distinct higher order amplitudes are particularly strong, representing the so called slotting harmonics [18], as for example of order $\nu = 36 \pm 2$ at the stator. To quantify how many members in terms of ν and n are needed to properly represent a field solution for these rather complicated boundary conditions, the analytical solutions shall now be compared to numerical results, which will be presented next.

The numerical model is implemented in COMSOL Multiphysics®. A structured quadrilateral mesh with quadratic ansatz functions is chosen and the numerical parameters are

$$r_1 = 1\,\mathrm{m}, \quad r_2 = 0.99\,r_1, \quad e = 0.5\,(r_1 - r_2), \quad \ell = 0.5\,\mathrm{m}.$$

As the results of this model shall provide a reference to the analytical solution they have to be sufficiently precise. A convergence study, where the number of mesh elements n_e is increased stepwise from 250 to 10000 guarantees this precision. Figures 6 a and b show the convergence of W_m^* and F_e with increasing n_e.

Evaluating the magnetic co-energy (eq. (20)) and its derivatives (eq. (21)) analytically requires calculating the sequence of integrals defined by eq. (18). Carrying out the convergence study, some interesting attributes of these sequences were
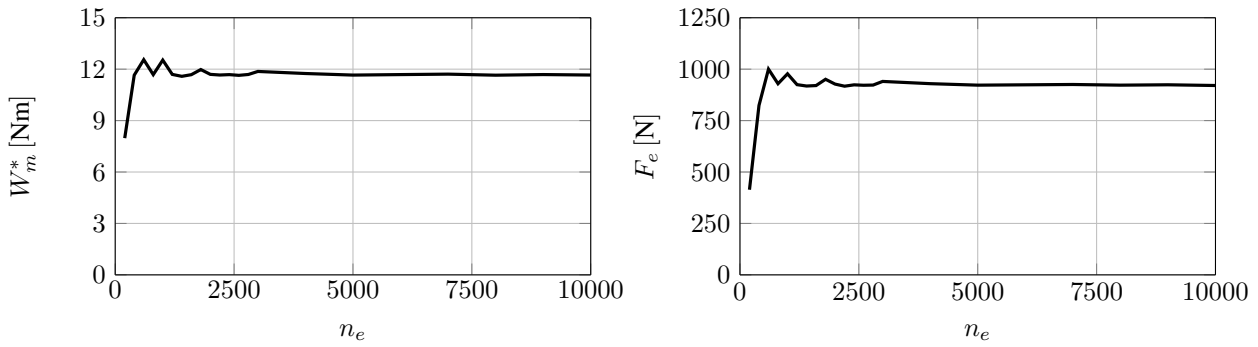
Figure 6: Convergence of numerical results with increasing number of elements.

found. Their behaviour can be explained considering figure 7, where the sequence $\mathcal{C}_{40,n}^{(1)}$ is plottet versus n for $\tau_1 = 1.31$. While the integral values are very low at the start, at about $n = \nu = 20$ some larger oscillations occur. With higher values of n they disappear and the sequence converges towards zero. Although showing only one example here, the qualitative behaviour is found to be equivalent for all sequences. In general, the oscillations appear at a certain range around $\nu = n$. From a numerical point of view, these sequences evoke some problems, as it is likely that numerical errors cause the sequence to diverge. This problem is overcome by increasing the numerical precision in this work but should be discussed in more detail, when higher orders n and ν are considered.
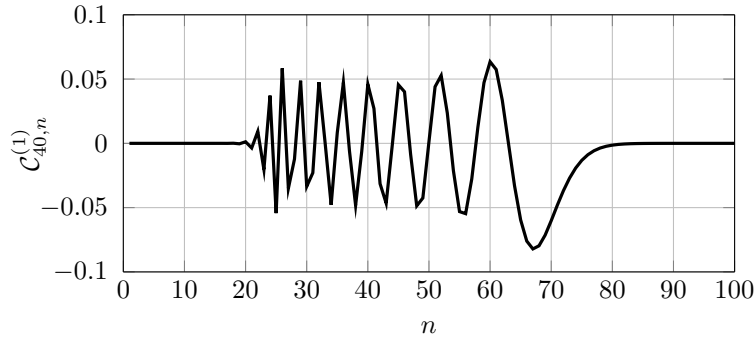

Figure 7: Sequence of integrals $\mathcal{C}_{40,n}^{(1)}$ for $\tau_1 = 1.31$.

However, being able to evaluate the sequence of integrals one is able to compare the analytical solution to numerical results. In this work, this is done by means of relative errors defined by

$$\mathcal{E}_{W_m^*} = \frac{|W_m^* - W_{m,num}^*|}{W_{m,num}^*} \quad \text{and} \quad \mathcal{E}_{F_e} = \frac{|F_e - F_{e,num}|}{F_{e,num}}. \tag{23}$$

Figure 8 shows these error measures as a function of the number of harmonics ν and n considered. Note that the result is given as a percentage and on a logarithmic scale. As one can see from figure 8, the magnetic energy converges very fast with a relative error below 1% for about 5 harmonics in ν and n. Certainly a further error drop can be observed at about $\nu = 36$, when the slotting harmonics are regarded.
The magnetic force also converges fast for low ν and n with an error below 1% at 5 harmonics each, but slightly oscillates when increasing n. These oscillations might be due to numerical problems computing the derivatives of the integrals in eq. (18).

In general, this convergence study shows the applicability of the approach for nonlinear rotordynamics of electrical machines. Having determined a solution to the magnetic field problem, forces and flux linkages can be calculated very fast and precisely. In fact, calculating the magnetic co-energy and its derivatives analytically is much faster than solving the task numerically and can also be much more precise if a sufficient number of harmonics is regarded. This property makes the method promising for coupling nonlinear field computation in the iron parts of the machine with the analytical solution found for the air gap.
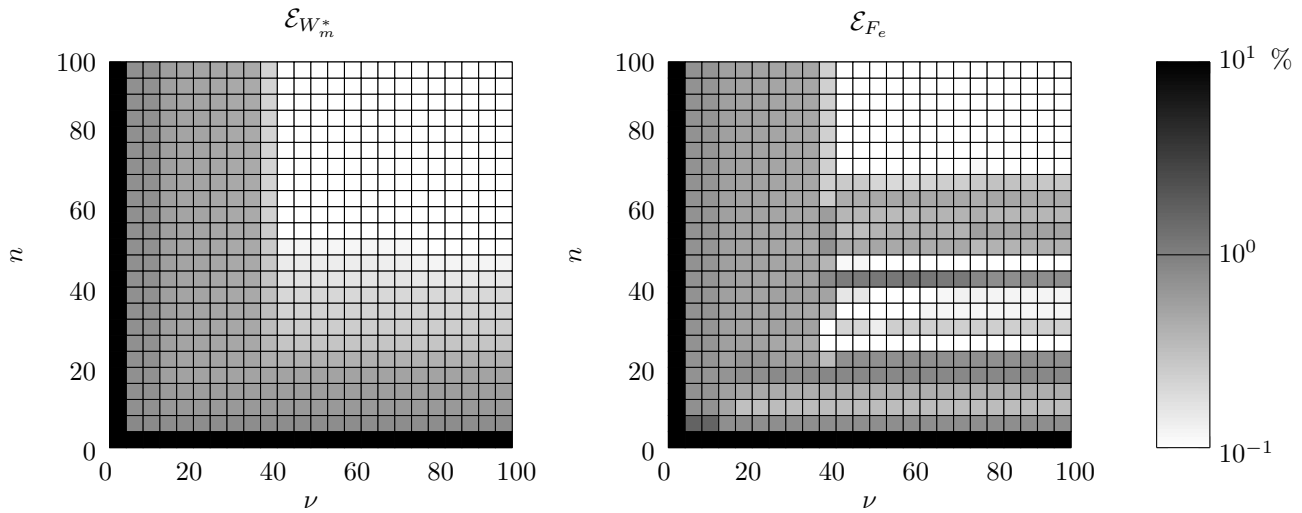
Figure 8: Convergence of analytical results.

Summary and Conclusions

Within this contribution, common methods to solve the magnetic field problem in the air gap of electrical machines with eccentrically running rotor have been revised and an analytical approach porposed by Skubov and Shumakovich [14] has been extended towards arbitrary machine designs. The key idea has been to use bipolar coordinates solving the involved Laplace equation on an eccentric annulus. While the solution stated by Skubov and Shumakovich has been restricted to two pole machines regarding only the fundamental harmonic in the boundary condition, this work has extended it towards any number of pole pairs and harmonics in the boundary spectrum. This has been done by calculating the occuring Fourier coefficients iteratively. It has turned out that this iteration has an interesting convergence behaviour, demanding for a high numerical accuracy when evaluating it.

The established analytical solution has been verified by a convergence study compared to a FE-model. Taking the magnetic co-energy and induced magnetic force as a convergence measure, it has turned out that the solution converges very fast with errors below 1% for about 5 harmonics in the field solution and boundary spectrum, respectively. This result verifies the applicability of the proposed approach towards nonlinear rotordynamics, as forces and flux linkages can be derived very easily from the given magnetic co-energy.

Furthermore, the method can be extended towards fully coupled numerical models. In this context one could solve the nonlinear field problem in the stator and rotor numerically and couple both regions with the analytical solution in the air gap. Calculating forces and flux linkages semi-analytically would prevent issues like mesh deformation and mesh dependent forces. Reducing computation time drastically, it could be used to carry out fully coupled electromechanical simulations. Under these circumstances the backcoupling between vibrations of the stator housing and the lateral rotor motion could be taken into account efficiently.

Appendix

Within this appendix, a brief discussion on the derivation of the Fourier coefficients, defined by eq. (16) shall be given. Inserting the boundary functions (15) into them, one finds out, that the basic task is to solve four kinds of integrals

$$-\frac{\sinh \tau_i}{\pi} \int_{-\pi}^{\pi} \begin{Bmatrix} \cos(\nu\theta_i) \\ \sin(\nu\theta_i) \end{Bmatrix} \begin{Bmatrix} \cos(n\sigma) \\ \sin(n\sigma) \end{Bmatrix} \frac{\mathrm{d}\sigma}{\cosh\tau_i - \cos\sigma} = \frac{1}{\pi} \int_{-\pi}^{\pi} \begin{Bmatrix} \cos(\nu\theta_i) \\ \sin(\nu\theta_i) \end{Bmatrix} \begin{Bmatrix} \cos(n\sigma) \\ \sin(n\sigma) \end{Bmatrix} \mathrm{d}\theta_i. \qquad (24)$$

As a first point it is easy to see, that integrals involving cosine and sine combinations are zero. The other ones shall be denoted by $\mathcal{C}_{\nu,n}^{(i)}$ and $\mathcal{S}_{\nu,1}^{(i)}$ as defined in eq. (17).

As the sequence for their solution in eq. (18) starts with $\mathcal{C}_{\nu,0}^{(i)}$ and $\mathcal{C}_{\nu,1}^{(i)}$, these expressions will be considered first. While $\mathcal{C}_{\nu,0}^{(i)} = 0$ is obvious, finding $\mathcal{C}_{\nu,1}^{(i)}$ involves some algebra. As a first step $\cos\sigma = \frac{1 - \cos\theta_i \cosh\tau_1}{\cosh\tau_i - \cos\theta_i}$ is replaced as a function of θ_i, resulting in

$$\mathcal{C}_{\nu,1}^{(i)} = \frac{1}{\pi} \int_{-\pi}^{\pi} \cos(\nu\theta_i) \cos\sigma \, \mathrm{d}\theta_i = -\frac{\sinh^2 \tau_i}{\pi} \int_{-\pi}^{\pi} \frac{\cos(\nu\theta_i)}{\cosh\tau_i - \cos\theta_i} \, \mathrm{d}\theta_i. \qquad (25)$$

Using Euler's formula for $\cos\theta_i$ and the substitution $x = e^{j\theta_i}$ one finds

$$\mathcal{C}_{\nu,1}^{(i)} = \frac{\sinh^2\tau_i}{j\pi} \int_{x(-\pi)}^{x(\pi)} \frac{x^\nu + x^{-\nu}}{(x-x_-)(x-x_-)}\, dx, \tag{26}$$

where $x_\pm = \cosh\tau_i \pm \sinh\tau_i$. This integral can be solved using partial fraction expansion resulting in

$$\mathcal{C}_{\nu,1}^{(i)} = 2\sinh\tau_i\big((\sinh\tau_i - \cosh\tau_i)U_{\nu-1}(\cosh\tau_i) + U_{\nu-2}(\cosh\tau_i)\big) = -2\sinh\tau_i e^{-\nu\tau_i}, \tag{27}$$

where U_ν are Chebyshev polynomials of the second kind.

Having determined the first two elements of the sequence, one can proceed applying integration by parts for $\mathcal{C}_{\nu,n}^{(i)}$ and $\mathcal{S}_{\nu,n}^{(i)}$. With the identity

$$\frac{d}{d\theta_i}\cos(n\sigma) = -n\sin(n\sigma)\frac{d\sigma}{d\theta_i} = n\sin(n\sigma)\frac{\cosh\tau_i - \cos\sigma}{\sinh\tau_i} \tag{28}$$

and by using some addition theorems, one finally finds the sequence in eq. (18) as well as $\mathcal{S}_{\nu,n}^{(i)} = -\mathcal{C}_{\nu,n}^{(i)}$.

References

[1] Früchtenicht J., Seinsch H.O. (1982) Exzentrizitätsfelder als Ursache von Laufinstabilitäten bei Asynchronmaschinen. *Electrical Engineering (Archiv für Elektrotechnik)* **65.4-5**: 271 - 281.

[2] Lakshmikanth S. (2012) Noise and Vibration Reduction in PMSM - A Review. *International Journal of Electrical and Computer Engineering* **2.3**: 405.

[3] Henao H. (2014) Trends in fault diagnosis for electrical machines: a review of diagnostic techniques. *IEEE industrial electronics magazine* **8.2**: 31-42.

[4] Silval B. et al. (2014) Computation of Torque of an Electrical Machine With Different Types of Finite Element Mesh in the Air Gap. *IEEE Transactions on Magnetics* **50.12**: 1-9.

[5] Rosenberg E. (1917) Einseitiger magnetischer Zug in elektrischen Maschinen. *Elektrotechnik und Maschinenbau* **35**: 525-531.

[6] Krondl M. (1956) Selbsterregte Rüttelschwingungen von Induktionsmaschinen mit parallelen Wicklungszweigen. *Bull. SEV* **17**: 581-588.

[7] Frohne H. (1968) Über den einseitigen magnetischen Zug in Drehfeldmaschinen. *Electrical Engineering (Archiv für Elektrotechnik)* **51**: 300-308.

[8] Jordan, H., Schroeder, R.-D., Seinsch, H. (1981) Zur Berechnung einseitigmagnetischer Zugkräfte in Drehfeldmaschienen. *Electrical Engineering (Archiv für Elektrotechnik)* **63**: 117-124.

[9] Belmans, R., Vandenput, A., Geysen, W. (1987) Calculation of the flux density and the unbalanced pull in two pole induction machines. *Electrical Engineering (Archiv für Elektrotechnik)* **70**: 151-161.

[10] Dorrell, D. G. (1993) Calculation of unbalanced magnetic pull in cage induction machines. PhD-Thesis, University of Cambridge.

[11] Werner U. (2006) Rotordynamische analyse von asynchronmaschinen mit magnetischen unsymmetrien. PhD-Thesis, Technische Universität Darmstadt.

[12] Boy F., Hetzler H. (2017) An Asymptotic Approximation of the Magnetic Field and Forces in Electrical Machines with Rotor Eccentricity. *Electrical Engineering* (online first version).

[13] Buchholz H. (1933) Die mechanischen Kräfte auf den exzentrisch rotierenden, zylindrischen Läufer einer zweipoligen Drehfeldmaschine mit flächenhaft verteilten Strombelägen. *Electrical Engineering (Archiv für Elektrotechnik)* **27**: 423-447.

[14] Skubov D., Shumakovich , I. (1999) Stability of the rotor of an induction machine in the magnetic field of the current windings. *Mechanics of solids* **34**: 28-40.

[15] Boyd J.P. (2013) Chebyshev and Fourier spectral methods. Dover Publications, Mineola, New York.

[16] Heyda J.F. (1959) A green's function solution for the case of laminar incompressible flow between non-concentric circular cylinders. *Journal of the Franklin Institute* **267.1**: 25-34.

[17] Binder A. (2012) Elektrische Maschinen und Antriebe [Electrical machines and drives]. Springer, Heidelberg.

[18] Haase H. (1973) Über die Störung der Laufruhe von Drehstromasynchronmaschinen infolge elektromagnetischer Anfachungen. PhD-Thesis, Technische Universität Hannover.